

Mutations in *SPATA7* Cause Leber Congenital Amaurosis and Juvenile Retinitis Pigmentosa

Hui Wang,^{1,7} Anneke I. den Hollander,^{10,11} Yalda Moayed, ³ Abuduaini Abulimiti,^{1,7} Yumei Li,^{1,7} Rob W.J. Collin,¹⁰ Carel B. Hoyng,¹¹ Irma Lopez,¹² Molly Bray,⁸ Richard Alan Lewis,^{1,2,9} James R. Lupski,^{1,5,9} Graeme Mardon,^{1,2,3,4,6} Robert K. Koenekoop,¹² and Rui Chen^{1,6,7,*}

Leber congenital amaurosis (LCA) and juvenile retinitis pigmentosa (RP) are the most common hereditary causes of visual impairment in infants and children. Using homozygosity mapping, we narrowed down the critical region of the *LCA3* locus to 3.8 Mb between markers *D14S1022* and *D14S1005*. By direct Sanger sequencing of all genes within this region, we found a homozygous nonsense mutation in the *SPATA7* gene in Saudi Arabian family KKESH-060. Three other loss-of-function mutations were subsequently discovered in patients with LCA or juvenile RP from distinct populations. Furthermore, we determined that *Spata7* is expressed in the mature mouse retina. Our findings reveal another human visual-disease gene that causes LCA and juvenile RP.

Introduction

Leber congenital amaurosis (LCA [MIM 204000]) is a set of inherited, early-onset retinal dystrophies that affect approximately 1:50,000 people in the general U.S. population and account for more than 5% of all retinal dystrophies.^{1,2} The clinical phenotypes of LCA are characterized by severe visual loss at birth, nystagmus, a variety of fundus changes, and minimal or absent recordable responses on the electroretinogram (ERG), usually with an autosomal-recessive pattern of inheritance.³ Consistent with this clinical variability, the molecular basis for LCA is also heterogeneous, with mutations described in fourteen genes. Functional studies of previously identified genes indicate that they act in strikingly diverse functional pathways underlying the disease, including retina development (*CRB1* [MIM 604210],⁴ *CRX* [MIM 602225]⁵⁻⁷), phototransduction (*GUCY2D* [MIM 600179],⁸ *AIPL1* [MIM 604392]⁹), vitamin A metabolism (*RPE65* [MIM 180069],^{10,11} *LRAT* [MIM 604863],¹² *RDH12* [MIM 608830]¹³), and cilium formation and function (*CEP290* [MIM 610142],¹⁴ *TULP1* [MIM 602280],¹⁵ *RPGRI1* [MIM 605446],^{16,17} *LCA5* [MIM 611408]¹⁸). In addition, the function of *RD3* remains unclear.¹⁹ Because of these profound differences in the underlying mechanisms of LCA, accurate molecular diagnosis of the disease is essential for the proper management of LCA patients. Therefore, identifying new genes and pathways and ascertaining the full complement of genes responsible for LCA are fundamental steps toward developing appropriate treatments for this devastating disease.

Knowledge obtained from LCA studies also offers insights into the pathogenesis and the molecular mechanisms underlying other retinal dystrophies, which are often shared.²⁰ LCA shares several important clinical

features with other retinal dystrophies, such as retinitis pigmentosa (RP [MIM 500004]). In fact, LCA was first described as an “intrauterine” form of RP.¹ Juvenile RP, unlike LCA, initially has a milder phenotype. It is often characterized by the onset of nyctalopia (night blindness), visual-field narrowing, and eventual visual-acuity loss, with or without nystagmus. Given the substantial clinical overlap with juvenile RP, it is expected that these two diseases might be caused by mutations in the same gene.²¹ Indeed, at least seven of the known LCA disease genes, including *CRX*, *CRB1*, *RPE65*, *RDH12*, *LRAT*, *MERTK*, and *TULP1*, have also been linked to the clinical appearance of juvenile RP in other families.²² Similarly, mutations in LCA genes may also be associated with other retinal diseases, such as cone-rod dystrophy (*CRX*,⁵ *AIPL1*,²³ and *GUCY2D*^{8,9}), and even systemic diseases, such as Joubert syndrome, Meckel syndrome, and Bardet-Biedl syndrome (*CEP290*²⁴⁻²⁶).

In addition to these 14 LCA genes, two genetic loci (*LCA3* at 14q24 and *LCA9* at 1p36) have been identified, but the underlying genes remain unknown.^{27,28} The exclusion of *RDH12* as an *LCA3* disease gene suggests that another retinal dystrophy disease gene is responsible for the *LCA3* phenotype.²⁹ In this report, we identified five new families that we mapped to the *LCA3* locus, utilizing fine mapping of the critical region through homozygosity mapping and single-nucleotide polymorphism (SNP) microarray technology.²¹ We identified homozygous nonsense and frameshift mutations in a positional candidate gene, *SPATA7* (spermatogenesis associated protein 7 [MIM 609868]) by direct Sanger sequencing. *SPATA7* encodes a highly conserved protein containing a single transmembrane domain. To better understand its normal function in the retina, we examined the expression pattern of *Spata7* in the developing

¹Department of Molecular and Human Genetics, ²Department of Ophthalmology, ³Department of Neuroscience, ⁴Department of Pathology, ⁵Department of Neurology, ⁶Program in Developmental Biology, ⁷Human Genome Sequencing Center, ⁸Children's Nutrition Research Center, ⁹Texas Children's Hospital, Baylor College of Medicine, Houston, TX 77030, USA; ¹⁰Department of Human Genetics, ¹¹Department of Ophthalmology, Nijmegen Centre for Molecular Life Sciences, Radboud University Nijmegen Medical Centre, 6500 HB Nijmegen, The Netherlands; ¹²McGill Ocular Genetics Center, McGill University Health Center, Montreal, Quebec H3H 1P3, Canada

*Correspondence: ruichen@bcm.edu

DOI 10.1016/j.ajhg.2009.02.005. ©2009 by The American Society of Human Genetics. All rights reserved.

and mature mouse retina, and we found that it is expressed in multiple retinal layers in the adult mouse retina.

Subjects and Methods

Study Subjects

We obtained blood samples and pedigrees after receiving informed consent from all individuals. Approval was obtained from the Institutional Review Boards of the participating centers. LCA families KKESH-019 and KKESH-060 were obtained by R.A.L. through the King Khaled Eye Specialist Hospital (KKESH) in Riyadh, Saudi Arabia. Blood samples were collected from all available family members, and DNA was extracted with the QIAGEN blood genomic DNA extraction kit, in accordance with the protocol provided by the manufacturer. Other LCA and juvenile RP samples were collected at the McGill University Health Center in Montreal or at the Department of Ophthalmology at the Radboud University Nijmegen Medical Centre in Nijmegen.

STR and SNP Genotyping and Sequencing

A list of microsatellite markers between D14S61 and D14S1015 were selected from the UCSC Human Genome Browser. For genotyping, primers specific for each marker were obtained from the human genome, and a universal tail was added to the 5' primer (5'-CTCGGTGCAGAGCATCATGC). PCR reactions were performed according to a standard protocol,³⁰ and products were size fractionated on an ABI 3700 capillary electrophoresis system and analyzed with the ABI GeneMapping software. A genome-wide scan of >318,000 tag SNPs was conducted on one affected member from the KKESH-060 and KKESH-019 families with the Illumina Hap300-Duo Bead Arrays, in accordance with the manufacturer's protocols. Homozygous regions were visualized and identified with the Bead Studio software package.

For identification of mutations in candidate genes, a direct PCR-sequencing approach was used. All exons and their splice junctions for each candidate gene (total of 9) in the critical *LCA3* region were amplified by PCR. The completeness and quality of the sequence was ensured by the design of primers from intron sequences so that the entire exon and at least 50 bp of intron DNA on each side of each exon were amplified for detection of potential mutations. For large exons, more than one pair of primers amplified overlapping regions spanning both the exon and its splice sites. Sequences for the primers of the 12 exons and splice junctions of *SPATA7* are included in Table S1 (available online).

Homozygosity Mapping with SNP Arrays for Identification of LCA and Juvenile RP Patients Whose Disease Region Overlaps with *LCA3*

We previously performed homozygosity mapping in 33 consanguineous and 60 nonconsanguineous individuals with LCA or juvenile RP from various ethnic origins with 10K, 100K, or 250K Affymetrix SNP microarrays,²¹ and we recently added 50 patients to this analysis (A.I.d.H., unpublished data). Five patients were found to be homozygous at the *LCA3* locus, with homozygous regions ranging in size from 1.6 to 29 Mb.

RNA In Situ Hybridization and Immunohistochemistry

An RNA in situ probe specific to *Spata7* (exons 8–12) was prepared according to a previously published protocol³¹ (probe 5'-primer:

5'-CTAATTACACGAGAAATGGTGCTG; probe 3'-primer: 5'-AGT GATGTGCTCAGACAACAGAGT). Total RNA was extracted from freshly isolated C57 wild-type (WT) eyes homogenized in Trizol (Invitrogen) and purified according to the manufacturer's instructions. A *Spata7* cDNA fragment was cloned into the *EcoRI* site of the TOPO cloning vector (Invitrogen). Antisense riboprobe constructs were linearized with *XhoI* and transcribed with SP6 RNA polymerase (DIG RNA Labeling Kit, Roche).

RNA in situ hybridization (ISH) and antibody staining was conducted on WT E16.5, P4, and P21 and C57Bl/6 129SvEv F1 hybrid eye sections. WT eyes were collected, fixed in 4% paraformaldehyde overnight, dehydrated in ethanol, and paraffin embedded. For ISH, 5 μ m eye sections were cut, dewaxed in xylene, then rehydrated and treated with proteinase K. Hybridization incubations were carried out in hybridization buffer (50% formamide, 5XSSC [pH 4.5–5.0], 1% SDS, 50 mg/ml yeast tRNA, 50 mg/ml heparin) at 65°C overnight, followed by three 30-min washes with prewarmed washing buffer (50% formamide, 1XSSC [pH 4.5–5.0], 1% SDS) at 65°C. The slides were then incubated with alkaline phosphatase-conjugated anti-DIG (Roche) in 1× MABT (100 mM maleic acid, 150 mM NaCl, 0.1% Tween 20, pH 7.5), 2% BRB (Roche) and 10% goat serum overnight at room temperature. After five washes (30 min each) with MABT buffer and one wash with NTMT (100 mM Tris-HCl [pH 9.5], 100 mM NaCl, 50 mM MgCl₂, 0.1% Tween 20, and 0.048% levamisole), hybridization signals were visualized by incubation with BM Purple (Roche) at room temperature for the desired time.

For immunohistochemistry (IHC), antigen retrieval was performed by boiling of 10 μ m sections in 0.01 M citrate buffer twice for 2 min, followed by cooling for 40 min at room temperature. Slides were washed in PBS, incubated for 1 hr at room temperature in hybridization buffer (10% normal goat serum, 0.1% Triton X-100, PBS), then incubated overnight in primary antibody diluted in hybridization buffer. Slides were then washed in PBS, incubated with secondary antibody diluted in hybridization buffer at room temperature for 2 hr, washed in PBS, and coverslipped. For testing the specificity of the *Spata7* antibody, a blocking experiment was performed. A GST-*Spata7* fusion protein was constructed by insertion of a mouse *Spata7* open reading frame into the multiple cloning site of the pGEX-4T-1 vector. The fusion protein was induced in the presence of 0.5 mM IPTG at 26°C for 8 hr and purified with the use of Glutathione Sepharose 4B as described in manufacturers' instructions (Amersham Bioscience). The in vitro antibody-depletion experiments were performed with purified GST or GST-*Spata7* fusion proteins bound to Glutathione Sepharose 4B. *Spata7* antibody was incubated with 50 μ l of GST beads, containing either GST-*Spata7* or GST, at 4°C overnight, then the depleted antibody was used for IHC as described above.

Dilutions and sources of antibodies were: mouse anti-rhodopsin (B6-30N) (1:100, a generous gift from W. Clay Smith), rabbit anti-*Spata7* (1:7.5, Proteintech Group), Alexa anti-mouse (1:400, Molecular Probes), Cy5 anti-rabbit (1:400, Jackson Immunochemicals). Fluorescent images were captured with a Zeiss LSM 510 confocal microscope and processed with Image J and Adobe Photoshop software.

Results

Fine Mapping of the *LCA3* Locus

Previously, the *LCA3* locus was mapped to chromosome 14q24 in a large, consanguineous LCA family (KKESH-019)

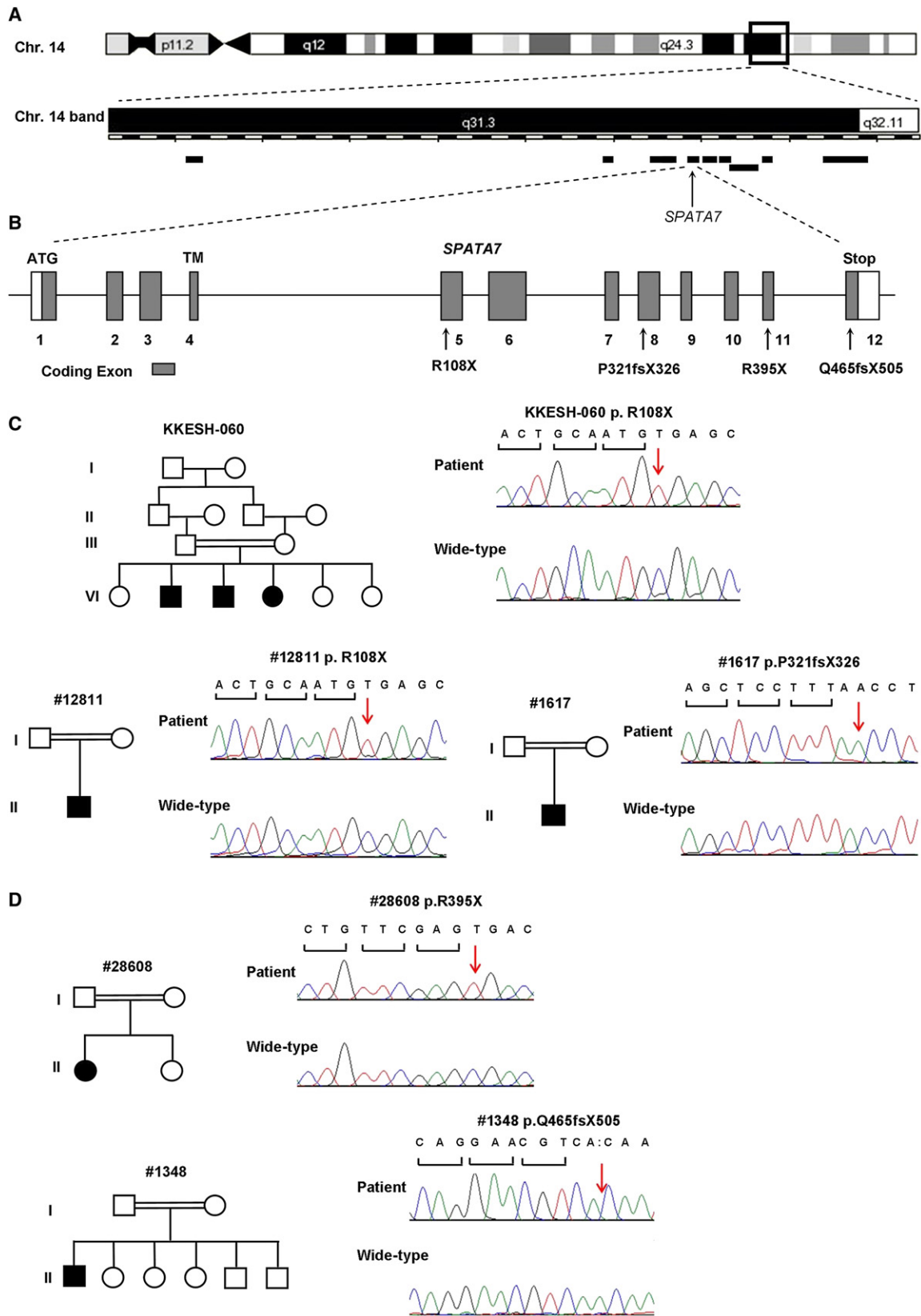


Figure 1. Mutations in *SPATA7* Cause LCA

(A) The *LCA3* critical interval at 14q31. Nine candidate genes within the region are indicated as black bars. *SPATA7* is indicated by a black arrow. The chromosome band is modified on the basis of the Ensemble ContigView.

(B) Exon-intron structure of the *SPATA7* gene is shown. Open boxes represent 5' and 3' UTRs, and solid boxes represent coding exons. A transmembrane domain (TM) is predicted to be encoded in exon 4. Mutations are indicated with arrows.

from Saudi Arabia with 15 affected and 42 unaffected members.²⁷ The critical region was initially identified by homozygosity mapping with STR markers. However, the distal boundary of the critical region was not well mapped, because there was no genotyping within a 10 Mb segment between *D14S74* and *D14S68*. More importantly, at least four recombinants have been reported for marker *D14S68*, indicating that the critical region could be greatly reduced by genotyping of additional markers within the distal region.

We therefore conducted fine mapping of the distal boundary of the critical region with additional STR markers between *D14S74* and *D14S68* (Table S1). On the basis of these genotyping results, all affected members of KKESH-019 were found to be homozygous between markers *D14S1022* and *D14S1005* (Figure S1). We then used these STR markers to scan additional LCA patient cohorts for new LCA families that may map to the *LCA3* region. In this manner, the KKESH-060 family from Saudi Arabia was also identified as an *LCA3* family²⁹ (Figure S2). All three affected members from the KKESH-060 family are homozygous from markers *D14S61* to *D14S1066*. To further confirm the homozygous region, DNA from one affected subject from each of these two families was genotyped by whole-genome SNP analysis with the Illumina SNP array. The new SNP genotyping results are consistent with the previous STR genotyping data, and affected subjects from these two families are homozygous for the *LCA3* locus at Chromosome 14q24 (Figure S3). Intersection of the homozygous region from these two LCA families defines a critical region of 3.8 Mb between markers *D14S1022* and *D14S1005*.

***SPATA7* Is Another LCA and Juvenile RP Gene**

A total of nine annotated genes are included within the newly defined *LCA3* critical region based on NCBI Build 36.1 (Figure 1A). Direct Sanger sequencing of all exons of all nine candidate genes from both *LCA3* families identified a nonsense mutation in *SPATA7*, a conserved gene containing 12 exons, in the KKESH-060 family (Figure 1C). All three affected members of KKESH-060 are homozygous for a nonsense mutation in the fifth exon (c.322C→T; p.R108X). The mutation segregates with the disease in this family, given that the three affected individuals are homozygous for the same mutation whereas the unaffected members are either heterozygous or do not carry the mutation (Figure 1C and Figure S2). Furthermore, the nonsense mutation is not a common SNP, because it is not recorded in the dbSNP database. Consistent with the above information, the mutation was not detected in 150 normal control samples, including 50 Saudi Arabian and

100 European samples, through direct sequencing of all exons of *SPATA7* (data not shown). No exonic mutation was found in KKESH-019 (see Discussion for details). To further confirm that *SPATA7* is an LCA disease gene, we sought to identify additional LCA patients with *SPATA7* mutations. By homozygosity mapping with genome-wide SNP microarrays, five additional patients with LCA or juvenile RP were recently found to be homozygous at the *LCA3* locus (²¹ and unpublished data). Mutation analysis of *SPATA7* revealed the same R108X nonsense mutation (found in the KKESH-060 family) in a Dutch LCA patient (no. 12811) (Figure 1C). On the basis of the STR genotyping result, the mutation analysis suggests that patient no. 12811 does not share the same haplotype with the patients from KKESH-060 (data not shown). This may be caused by a rapid decay of CpG sites, given that the 5-methylcytosine at CpG sites mutates unidirectionally to thymine by spontaneous deamination at a much higher transition rate compared to non-CpG dinucleotides.³² Finally, a homozygous frameshift mutation (c.961dupA; p.P321TfsX326) in exon 8 of *SPATA7* was found in an LCA patient (no. 1617) of Middle Eastern origin (Figure 1C). In addition, a Portuguese patient (no. 28608) with juvenile RP was found to be homozygous for a nonsense mutation (c.1183C→T; p.R395X) in exon 11 of *SPATA7* (Figure 1D). Finally, a homozygous frameshift mutation in exon 12 (c.1546delA; p.Q465fsX505) was identified in a French Canadian patient (no. 1348) with juvenile RP (Figure 1D). All mutations segregated with the disease in the affected families were not found in the 150 normal controls or in the SNP databases. In contrast to the two *SPATA7* mutations identified in LCA patients (p.R108X and p.P321TfsX326), the two juvenile RP mutations are close to the C-terminal part of the *SPATA7* protein.

Although carrying mutations in the same gene, the two juvenile RP patients present a clinical phenotype that is less severe than that of LCA patients. All three LCA patients from the KKESH-060 family showed poor visual fixation and function from birth and subsequently developed nystagmus, hyperopic astigmatism, and a nondetectable electroretinogram. A Dutch patient (no. 12811) was first seen in our clinic at age 6. She has had visual problems since birth, showing rotating nystagmus, peripheral chorio-retinal atrophy, and bone spicules pigmentation. In contrast, a 7-year-old Portuguese girl (no. 28608, diagnosed with juvenile RP) has excellent visual acuity (20/20), and nystagmus is absent. She developed early-onset nyctalopia before age 2 and has 5° visual fields (Goldmann) and nondetectable ERGs (Figure 2A). Similarly, a juvenile RP patient (no. 1348) from a French Canadian family was found to have hand-motion vision at age 55.

(C) Pedigrees and sequences of mutations of LCA families. Two different mutations were identified in these three families: all three patients from the KKESH-060 family, c.322C→T (p.R108X); patient no. 12811 from the Dutch family, c.322C→T (p.R108X); patient no. 1617 from the family with mid Eastern origin, c.961dupA (p.P321TfsX326).

(D) Pedigrees and sequences of mutations of juvenile RP families. Two different mutations were identified: patient no. 28608, c.1183C→T (p.R395X); patient no. 1348, c.1546delA (p.Q465fsX505).

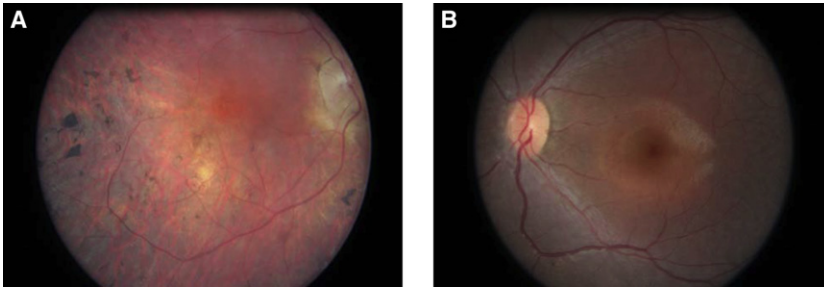


Figure 2. Color Photographs of the Retinas of Two RP Patients with *SPATA7* Mutations

(A) Retinal image of the right eye of a 55-year-old male with juvenile RP and a homozygous c.1546delA p.Q465fsX505 frameshift mutation in *SPATA7*.

(B) Retinal photograph of the left eye of a 9-year-old female with 20/20 acuities, 5° visual fields, and a homozygous p.R395X nonsense mutation in *SPATA7*. The retinal appearance shows narrow arterioles but normal-caliber

veins, normal color of the optic disc, a subtle grayish discoloration of the retina, and a faint hypopigmented diffuse perifoveal annulus. There were no pigmentary changes.

He reported seeing normally as a child and then declining, developing night blindness and nystagmus. This patient was found to have advanced retinal pigmentary degeneration, with narrow arterioles, optic disc pallor, and a small maculopathy on exam at age 55 years (Figure 2B). The ERG was nondetectable, and the visual fields were reduced to 5° with the V4e target.

***Spata7* Is a Highly Conserved, Vertebrate-Specific Protein Expressed in the Mature Retina**

Human *SPATA7* comprises 12 exons (Figure 1B) that encode a protein of 599 amino acids. *SPATA7* is conserved from sea urchin to human but is absent in lower eukaryotes, such as insects and fungi (Figure S4). A single-pass transmembrane domain is predicted by the PSIPred program (Figure 1B). However, no previously known functional domains have been identified.

Studies of gene-expression profiles, including the use of microarrays and databases of expressed sequence tags, indicate that *SPATA7* is expressed in the human retina. We examined the expression pattern of *Spata7* in the mouse retina at several developmental stages, using both mRNA ISH and IHC. Mouse retinas were stained at three developmental time points, E16.5, P4, and P21, corresponding to early, middle, and fully developed retinas. On the basis of the ISH results, *Spata7* is not detectable in the E16.5 or P4 mouse retina (Figures 3A and 3B), suggesting that *Spata7* is not required for early retinal development. In contrast, expression is observed in the P21 mature mouse retina, suggesting that *Spata7* may be involved in normal retinal function rather than development (Figure 3C). Consistent with ISH results, little *Spata7* protein is detected in the P4 mouse retina by IHC (Figures 3D–3F). In contrast, expression of *Spata7* protein is observed in multiple layers of the P21 retina, including the ganglion cell and inner nuclear layers, and inner segments of photoreceptors (Figures 3G–3L).

Discussion

It is interesting to note that mutations in *SPATA7* cause LCA and RP, two overlapping but distinct human retinal diseases. A fascinating aspect of human retinal diseases is the enormous heterogeneity in terms of both clinical

phenotypes and their underlying molecular mechanisms. Undoubtedly complex genetic inheritance contributes to this heterogeneity. For example, digenic triallelic inheritance has been observed in some families segregating the Bardet-Biedl phenotype, in which inheritance of a mutation in a second gene is required for an individual who has two mutations in the first gene to exhibit a clinical phenotype or to modify the severity of the primary phenotype.³³ Another major cause for heterogeneity is differential severity of mutant alleles at a single locus, as is likely in our study. We have isolated multiple loss-of-function mutations in *SPATA7* that cause either LCA or juvenile RP. Consistent with the observation that LCA has a more severe clinical phenotype than juvenile RP, the mutant alleles associated with LCA are likely to be more severe loss-of-function alleles than those associated with juvenile RP. The two alleles found in our LCA patients are nonsense mutations located in the middle of the *SPATA7* coding region (exons 5 and 8; Figure 1B). These two mutations will probably cause relatively early protein truncations and therefore are likely to be severe loss-of-function alleles because of nonsense-mediated decay and destruction of message.^{34,35} In contrast, the two mutations that we identified in the juvenile RP patients are located in the last two exons of *SPATA7*. Because these two mutations are very close to the C terminus of the protein, they will probably cause only truncation of a small portion of the protein product, although it is possible that the mutation in the second-to-last exon could cause a reduction of *SPATA7* mRNA levels as a result of nonsense-mediated decay.^{34,35} Therefore, our findings provide suggestive evidence of a correlation between the severity of mutant alleles in *SPATA7* and the resulting clinical phenotype.

It is conceivable that many human diseases are caused not only by coding mutations but by noncoding-region mutations that may affect gene expression. For example, the most prominent mutation in the LCA gene *CEP290* is an intron mutation that causes aberrant splicing of the transcript.¹⁴ Our data suggest that the initial *LCA3* family, KKESH-019, probably carries a mutation outside of the coding region of the *SPATA7* gene rather than in other genes in this locus. All genes within the critical region defined by the KKESH-019 family alone have been sequenced, and no mutations were identified within

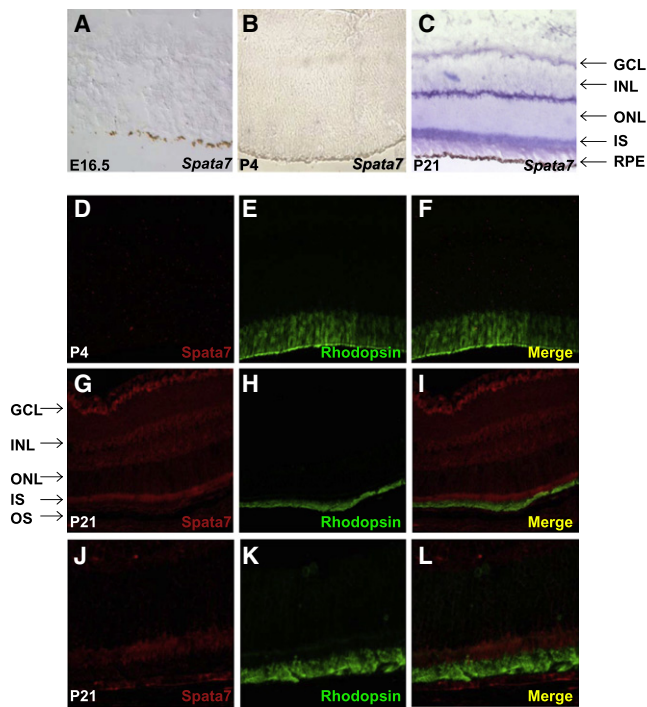


Figure 3. *Spata7* Is Expressed in the Adult Mouse Retina

(A–C) Section ISH with *Spata7* riboprobes. (A) *Spata7* is absent in all layers of the E16.5 mouse eye. (B) *Spata7* is absent in all layers of the P4 mouse eye. (C) At P21, *Spata7* is present in the ganglion cell layer, the inner nuclear layer, and the inner segment of the photoreceptors.

(D–F) Double immunostaining of *Spata7* (red) and Rhodopsin (green) shows that *Spata7* is not expressed in the P4 mouse retina.

(G–I) Double immunostaining of *Spata7* (red) and Rhodopsin (green) in the P21 mouse retina demonstrates that *Spata7* protein is expressed in multiple cell layers of the retina.

(J–L) High-magnification images of photoreceptors reveals that *Spata7* expression is prominent in the inner segment and sparse in the Rhodopsin-labeled outer segment. Abbreviations are as follows: ONL, outer nuclear layer; IS, inner segment; INL, inner nuclear layer; GCL, ganglion cell layer; RPE, retinal pigment epithelium; OS, outer segment.

exonic sequences in the KKESH-019 family. To identify a disease-causing mutation in the KKESH-019 family, we first sequenced the 5' and 3' UTR regions of *SPATA7*, but we found no change. Furthermore, to test for possible chromosome rearrangements at the *SPATA7* locus in this family, we used tiling of 3 kb PCR amplicons to analyze the entire *SPATA7* locus, including about 50 kb beyond the transcription unit, from an affected KKESH-019 patient, but we found no obvious changes compared to WT. This result suggests that no major chromosomal rearrangements, insertions, or deletions are present at the *SPATA7* locus in the KKESH-019 family. However, sequencing of these PCR products did identify several changes, including single-nucleotide substitutions and small insertions and deletions in the promoter region and introns of *SPATA7*. Because RNA samples from the KKESH-019 family are not available, we are not able to test

whether these changes can indeed affect *SPATA7* expression in the patients. Additional experiments will need to be carried to determine whether any of these noncoding changes cause defects in normal *SPATA7* expression.

SPATA7 is a gene that was first identified in human spermatocytes. On the basis of its expression pattern, *SPATA7* may be involved in preparing chromatin in early meiotic prophase nuclei for the initiation of meiotic recombination.³⁶ We found that in addition to its expression in testis, *Spata7* is expressed in multiple layers of the mature mouse retina. On the basis of its expression pattern in the retina, it would seem that *SPATA7* is not a typical cilium protein, despite its potential function in both sperm and retina. Close examination of *SPATA7* expression in the retina indicates that the protein is not enriched at the junction between the inner and outer segments of photoreceptor cells, where the cilium is located. Rather, the protein shows a uniform distribution in the cytoplasm of the inner segment. Given this information, together with the relatively late onset of *SPATA7* expression in the retina, we speculate that *SPATA7* may be involved a novel pathway. Additional studies need to be carried out to reveal the function of *SPATA7*.

In summary, we report the cloning of another LCA disease gene, *SPATA7*. The *LCA3* locus was first mapped to chromosome 14 more than 10 years ago, but the causal gene had not been identified. Through the combination of homozygosity mapping by SNP arrays and direct Sanger sequencing of all positional candidate genes within the *LCA3* critical region, we identified *SPATA7* as the disease-causing gene. Given that we identified multiple mutations in distinct ethnic groups, this gene appears to be an important player in LCA and in other retinal diseases, such as juvenile RP. As a gene that is linked to multiple human diseases, *SPATA7* offers opportunities for uncovering novel insights into human pathogenesis.

Supplemental Data

Supplemental Data include four figures and two tables and can be found with this article online at <http://www.ajhg.org/>.

Acknowledgments

We thank Huawei Xin for his help throughout this project and for his useful comments during the preparation of the manuscript. We are indebted to John Cavender, the Research Director of King Khalid Eye Specialist Hospital at the time of these studies, to the Research Council of KKESH for its financial support, and to the staff of its Research Department for their diligent commitment to this program. In addition, we thank the families reported here for their willing cooperation with these studies. R.A.L. is a Senior Scientific Investigator of Research to Prevent Blindness, New York. We also thank Frans Cremers for his valuable discussions and Lara Bou-Khizam for her technical assistance. This work is supported by grants from the Retinal Research Foundation and the National Eye Institute (R01EY018571) to R.C. R.K.K. is supported by the Foundation Fighting Blindness Canada and the

Fonds de la Recherche en Santee du Quebec (FRSQ). A.I.d.H. is supported by grants from the Netherlands Organisation for Scientific Research (916.56.160) and the Foundation Fighting Blindness USA (BR-GE-0606-0349-RAD).

Received: December 18, 2008

Revised: February 4, 2009

Accepted: February 6, 2009

Published online: March 5, 2009

Web Resources

The URLs for data presented herein are as follows:

Online Mendelian Inheritance in Man (OMIM), <http://www.ncbi.nlm.nih.gov/Omim/>

PSIPred program, <http://bioinf.cs.ucl.ac.uk/psipred/>

Retinal Information Network, <http://www.sph.uth.tmc.edu/Retnet/>

UCSC Human Genome Browser, <http://genome.ucsc.edu/index.html?org=Human&db=hg18&hsid=120774634>

References

1. Leber, T. (1869). Uber retinitis pigmentosa und angeborene amaurose. *Albrecht Von Graefes Arch. Ophthalmol.* 15, 1–25.
2. Dharmaraj, S.R., Silva, E.R., Pina, A.L., Li, Y.Y., Yang, J.M., Carter, C.R., Loyer, M.K., El-Hilali, H.K., Traboulsi, E.K., Sundin, O.K., et al. (2000). Mutational analysis and clinical correlation in Leber congenital amaurosis. *Ophthalmic Genet.* 21, 135–150.
3. Lewis, R.A. (1988). *Juvenile Hereditary Macular Dystrophies* (New York: Retinal Dystrophies and Degenerations. Raven Press), 115–134.
4. den Hollander, A.I., Heckenlively, J.R., van den Born, L.I., de Kok, Y.J., van der Velde-Visser, S.D., Kellner, U., Jurklics, B., van Schooneveld, M.J., Blankenagel, A., Rohrschneider, K., et al. (2001). Leber congenital amaurosis and retinitis pigmentosa with Coats-like exudative vasculopathy are associated with mutations in the crumbs homologue 1 (CRB1) gene. *Am. J. Hum. Genet.* 69, 198–203.
5. Freund, C.L., Wang, Q.L., Chen, S., Muskat, B.L., Wiles, C.D., Sheffield, V.C., Jacobson, S.G., McInnes, R.R., Zack, D.J., and Stone, E.M. (1998). De novo mutations in the CRX homeobox gene associated with Leber congenital amaurosis. *Nat. Genet.* 18, 311–312.
6. Swaroop, A., Wang, Q.L., Wu, W., Cook, J., Coats, C., Xu, S., Chen, S., Zack, D.J., and Sieving, P.A. (1999). Leber congenital amaurosis caused by a homozygous mutation (R90W) in the homeodomain of the retinal transcription factor CRX: direct evidence for the involvement of CRX in the development of photoreceptor function. *Hum. Mol. Genet.* 8, 299–305.
7. Jacobson, S.G., Cideciyan, A.V., Huang, Y., Hanna, D.B., Freund, C.L., Affatigato, L.M., Carr, R.E., Zack, D.J., Stone, E.M., and McInnes, R.R. (1998). Retinal degenerations with truncation mutations in the cone-rod homeobox (CRX) gene. *Invest. Ophthalmol. Vis. Sci.* 39, 2417–2426.
8. Perrault, I., Rozet, J.M., Calvas, P., Gerber, S., Camuzat, A., Dollfus, H., Chatelin, S., Souied, E., Ghazi, I., Leowski, C., et al. (1996). Retinal-specific guanylate cyclase gene mutations in Leber's congenital amaurosis. *Nat. Genet.* 14, 461–464.
9. Sohocki, M.M., Bowne, S.J., Sullivan, L.S., Blackshaw, S., Cepko, C.L., Payne, A.M., Bhattacharya, S.S., Khaliq, S., Qasim Mehdi, S., Birch, D.G., et al. (2000). Mutations in a new photoreceptor-pineal gene on 17p cause Leber congenital amaurosis. *Nat. Genet.* 24, 79–83.
10. Marlhens, F., Bareil, C., Griffoin, J.M., Zrenner, E., Amalric, P., Eliaou, C., Liu, S.Y., Harris, E., Redmond, T.M., Arnaud, B., et al. (1997). Mutations in RPE65 cause Leber's congenital amaurosis. *Nat. Genet.* 17, 139–141.
11. Perrault, I., Rozet, J.M., Ghazi, I., Leowski, C., Bonnemaïson, M., Gerber, S., Ducroq, D., Cabot, A., Souied, E., Dufier, J.L., et al. (1999). Different functional outcome of RetGC1 and RPE65 gene mutations in Leber congenital amaurosis. *Am. J. Hum. Genet.* 64, 1225–1228.
12. Thompson, D.A., Li, Y., McHenry, C.L., Carlson, T.J., Ding, X., Sieving, P.A., Apfelstedt-Sylla, E., and Gal, A. (2001). Mutations in the gene encoding lecithin retinol acyltransferase are associated with early-onset severe retinal dystrophy. *Nat. Genet.* 28, 123–124.
13. Janecke, A.R., Thompson, D.A., Utermann, G., Becker, C., Hubner, C.A., Schmid, E., McHenry, C.L., Nair, A.R., Ruschendorf, F., Heckenlively, J., et al. (2004). Mutations in RDH12 encoding a photoreceptor cell retinol dehydrogenase cause childhood-onset severe retinal dystrophy. *Nat. Genet.* 36, 850–854.
14. den Hollander, A.I., Koenekoop, R.K., Yzer, S., Lopez, I., Arends, M.L., Voeselek, K.E., Zonneveld, M.N., Strom, T.M., Meitinger, T., Brunner, H.G., et al. (2006). Mutations in the CEP290 (NPHP6) gene are a frequent cause of Leber congenital amaurosis. *Am. J. Hum. Genet.* 79, 556–561.
15. Hagstrom, S.A., North, M.A., Nishina, P.L., Berson, E.L., and Dryja, T.P. (1998). Recessive mutations in the gene encoding the tubby-like protein TULP1 in patients with retinitis pigmentosa. *Nat. Genet.* 18, 174–176.
16. Gerber, S., Perrault, I., Hanein, S., Barbet, F., Ducroq, D., Ghazi, I., Martin-Coignard, D., Leowski, C., Homfray, T., Dufier, J.L., et al. (2001). Complete exon-intron structure of the RPGR-interacting protein (RPGRIP1) gene allows the identification of mutations underlying Leber congenital amaurosis. *Eur. J. Hum. Genet.* 9, 561–571.
17. Dryja, T.P., Adams, S.M., Grimsby, J.L., McGee, T.L., Hong, D.H., Li, T., Andreasson, S., and Berson, E.L. (2001). Null RPGRIP1 alleles in patients with Leber congenital amaurosis. *Am. J. Hum. Genet.* 68, 1295–1298.
18. den Hollander, A.I., Koenekoop, R.K., Mohamed, M.D., Arts, H.H., Boldt, K., Towns, K.V., Sedmak, T., Beer, M., Nagel-Wolfrum, K., McKibbin, M., et al. (2007). Mutations in LCA5, encoding the ciliary protein lebercilin, cause Leber congenital amaurosis. *Nat. Genet.* 39, 889–895.
19. Friedman, J.S., Chang, B., Kannabiran, C., Chakarova, C., Singh, H.P., Jalali, S., Hawes, N.L., Branham, K., Othman, M., Filippova, E., et al. (2006). Premature truncation of a novel protein, RD3, exhibiting subnuclear localization is associated with retinal degeneration. *Am. J. Hum. Genet.* 79, 1059–1070.
20. Lewis, R.A., Allikmets, R., and Lupski, J.R. (2001). Inherited macular dystrophies and susceptibility to degeneration. In *The Metabolic and Molecular Bases of Inherited Diseases*, Eighth Edition, C.R. Scriver, A.L. Beaudet, W.S. Sly, D. Valle, B. Childs, and B. Vogelstein, eds. (New York: McGraw-Hill), pp. 6077–6096.
21. den Hollander, A.I., Lopez, I., Yzer, S., Zonneveld, M.N., Jansen, I.M., Strom, T.M., Hehir-Kwa, J.Y., Veltman, J.A., Arends, M.L., Meitinger, T., et al. (2007). Identification of novel mutations in patients with Leber congenital amaurosis and juvenile

- RP by genome-wide homozygosity mapping with SNP microarrays. *Invest. Ophthalmol. Vis. Sci.* **48**, 5690–5698.
22. den Hollander, A.I., Roepman, R., Koenekoop, R.K., and Cremers, F.P. (2008). Leber congenital amaurosis: genes, proteins and disease mechanisms. *Prog. Retin. Eye Res.* **27**, 391–419.
 23. Sohocki, M.M., Perrault, I., Leroy, B.P., Payne, A.M., Dharmaraj, S., Bhattacharya, S.S., Kaplan, J., Maumenee, I.H., Koenekoop, R., Meire, F.M., et al. (2000). Prevalence of AIPL1 mutations in inherited retinal degenerative disease. *Mol. Genet. Metab.* **70**, 142–150.
 24. Valente, E.M., Silhavy, J.L., Brancati, F., Barrano, G., Krishnaswami, S.R., Castori, M., Lancaster, M.A., Boltshauser, E., Boccone, L., Al-Gazali, L., et al. (2006). Mutations in CEP290, which encodes a centrosomal protein, cause pleiotropic forms of Joubert syndrome. *Nat. Genet.* **38**, 623–625.
 25. Baala, L., Audollent, S., Martinovic, J., Ozilou, C., Babron, M.C., Sivanandamoorthy, S., Saunier, S., Salomon, R., Gonzales, M., Rattenberry, E., et al. (2007). Pleiotropic effects of CEP290 (NPHP6) mutations extend to Meckel syndrome. *Am. J. Hum. Genet.* **81**, 170–179.
 26. Leitch, C.C., Zaghoul, N.A., Davis, E.E., Stoetzel, C., Diaz-Font, A., Rix, S., Alfadhel, M., Lewis, R.A., Eyaid, W., Banin, E., et al. (2008). Hypomorphic mutations in syndromic encephalocoele genes are associated with Bardet-Biedl syndrome. *Nat. Genet.* **40**, 443–448.
 27. Stockton, D.W., Lewis, R.A., Abboud, E.B., Al-Rajhi, A., Jabak, M., Anderson, K.L., and Lupski, J.R. (1998). A novel locus for Leber congenital amaurosis on chromosome 14q24. *Hum. Genet.* **103**, 328–333.
 28. Keen, T.J., Mohamed, M.D., McKibbin, M., Rashid, Y., Jafri, H., Maumenee, I.H., and Inglehearn, C.F. (2003). Identification of a locus (LCA9) for Leber's congenital amaurosis on chromosome 1p36. *Eur. J. Hum. Genet.* **11**, 420–423.
 29. Li, Y., Wang, H., Peng, J., Gibbs, R.A., Lewis, R.A., Lupski, J.R., Mardon, G., and Chen, R. (2008). Mutation survey of known LCA genes and loci in the Saudi Arabian population. *Invest. Ophthalmol. Vis. Sci.* Published online October 20, 2008.
 30. Guo, D.C., and Milewicz, D.M. (2003). Methodology for using a universal primer to label amplified DNA segments for molecular analysis. *Biotechnol. Lett.* **25**, 2079–2083.
 31. Wilkinson, D.G., and Nieto, M.A. (1993). Detection of messenger RNA by in situ hybridization to tissue sections and whole mounts. *Methods Enzymol.* **225**, 361–373.
 32. Coulondre, C., Miller, J.H., Farabaugh, P.J., and Gilbert, W. (1978). Molecular basis of base substitution hotspots in *Escherichia coli*. *Nature* **274**, 775–780.
 33. Katsanis, N., Eichers, E.R., Ansley, S.J., Lewis, R.A., Kayserili, H., Hoskins, B.E., Scambler, P.J., Beales, P.L., and Lupski, J.R. (2002). BBS4 is a minor contributor to Bardet-Biedl syndrome and may also participate in triallelic inheritance. *Am. J. Hum. Genet.* **71**, 22–29.
 34. Inoue, K., Khajavi, M., Ohyama, T., Hirabayashi, S., Wilson, J., Reggin, J.D., Mancias, P., Butler, I.J., Wilkinson, M.F., Wegner, M., et al. (2004). Molecular mechanism for distinct neurological phenotypes conveyed by allelic truncating mutations. *Nat. Genet.* **36**, 361–369.
 35. Khajavi, M., Inoue, K., and Lupski, J.R. (2006). Nonsense-mediated mRNA decay modulates clinical outcome of genetic disease. *Eur. J. Hum. Genet.* **14**, 1074–1081.
 36. Zhang, X., Liu, H., Zhang, Y., Qiao, Y., Miao, S., Wang, L., Zhang, J., Zong, S., and Koide, S.S. (2003). A novel gene, RSD-3/HSD-3.1, encodes a meiotic-related protein expressed in rat and human testis. *J. Mol. Med.* **81**, 380–387.